Chemical Physics Letters 500 (2010) 291–294

Contents lists available at ScienceDirect

Chemical Physics Letters

journal homepage: www.elsevier.com/locate/cplett

Desorption of H atoms from graphite (0001) using XUV free electron laser pulses

B. Siemer [a,*], T. Olsen [b], T. Hoger [a], M. Rutkowski [a], C. Thewes [a], S. Düsterer [c], J. Schiøtz [b], H. Zacharias [a]

[a] Physikalisches Institut, Westfälische Wilhelms-Universität Münster, Wilhelm Klemm Str. 10, 48149 Münster, Germany
[b] Danish National Research Foundation's Center of Individual Nanoparticle Functionality (CINF), Department of Physics, Technical University of Denmark, DK-2800 Kongens Lyngby, Denmark
[c] HASYLAB, Deutsches Elektronen Synchotron, Notkestr. 85, 22607 Hamburg, Germany

ARTICLE INFO

Article history:
Received 6 July 2010
In final form 18 October 2010
Available online 20 October 2010

ABSTRACT

The desorption of neutral H atoms from graphite with femtosecond XUV pulses is reported. The velocity distribution of the atoms peaks at extremely low kinetic energies. A DFT-based electron scattering calculation traces this distribution to desorption out of specific adsorption sites on graphite, and identifies the highest vibrational state in the adsorbate potential as a major source for the slow atoms. It is evident that multiple electron scattering processes are required for this desorption. A direct electronic excitation of a repulsive hydrogen–carbon bond seems not to be important.

1. Introduction

Photochemically triggered reactions on dust grains are considered to be a major source of molecule formation in interstellar clouds. These grains typically consist of graphitic and silicate particles and conglomerates, in the central regions of the clouds often covered with icy layers. In warmer parts of the clouds which are irradiated by newly born stars and in the accretion discs of such stars most of the ice layers have evaporated, and bare grains are exposed [1]. The reaction dynamics of hydrogen constitutes the one of the more important reactions. Such reactions on graphite or graphene sheets gained considerable interest recently, as they are accompanied with a considerable change in the local electronic structure.

Upon chemical binding of atomic hydrogen the generally sp^2 bound carbon scaffold of graphene is locally distorted. The now binding C atom develops an sp^3 hybridization, and puckers out of the graphite plane by about 0.3 Å. This electronic change and the atomic movement cause a barrier in the adsorption pathway of about 0.25 eV [2,3]. The H atoms then bind with an energy of about $E_b \sim 0.85$ eV. Co-adsorption of a second H atom in the vicinity of an already adsorbed one is preferred on the next-neighbor ortho position and on the so-called para position on the opposite site of the carbon hexagons, as was confirmed by scanning tunnelling microscopy [4]. In these two positions the binding energy increases to 1.9–2.1 eV, while in the nearest next neighbor (meta) position it remains unchanged. In both positions the adsorption barrier is reduced, for para adsorption even to zero energy. Correspondingly, preferential reaction sites exist for thermal molecular hydrogen formation out of these pre-paired H atoms [5,6].

Recently, femtosecond laser induced desorption of atomic hydrogen from graphite has been observed with near-UV radiation of 3.1 eV photon energy [7]. Distinct features in the velocity distribution could be assigned to desorption out of the mentioned pre-paired preferential ortho and para adsorption sites. In this Letter we report on first results obtained after irradiation of the surface system with femtosecond extreme ultraviolet (XUV) pulses provided by the free-electron laser at Hamburg (FLASH) at DESY. The photon energy chosen ($h\nu = 38$ eV) is close to the HeII resonance line. This high photon energy in principle enables a direct electronic excitation of the hydrogen graphite bond, but also the creation of a hot electron gas in the graphite substrate.

2. Experimental

The experiment is carried out at the free-electron laser at Hamburg (FLASH) at DESY which provides radiation in the XUV and soft X-ray regime from about 20 eV to 206 eV in the fundamental on the unmonochromatized beamline BL1 [8]. The highly oriented pyrolytic graphite (HOPG) sample is placed on a manipulator mounted in a UHV chamber with a base pressure of 2×10^{-10} mbar. The sample is cleaned by cleaving the top layers just before placing it into the chamber and heading up to ~850 K for prolonged time to remove any adsorbates. For atomic hydrogen adsorption and the experiment the sample is cooled to a temperature of $T_s = 300$ K. Hydrogen atoms are produced by thermal dissociation in a tungsten capillary heated to more than 2200 K. The capillary has a distance of 80 mm from the sample. During H atom adsorption the chamber pressure rises up to 8×10^{-8} mbar for ca. 60 min, which corresponds to a coverage of 0.4 ML. The desorption laser FLASH operates at 5 Hz repetition rate in a single bunch mode at a photon energy of $h\nu = 38.8$ eV ($\lambda = 32.0$ nm) with a temporal pulse width of about 30 fs [9]. The weakly focused p̂-polarized XUV

* Corresponding author. Fax: +49 251 83 33604.
E-mail address: b.siemer@uni-muenster.de (B. Siemer).

0009-2614/$ - see front matter © 2010 Elsevier B.V. All rights reserved.
doi:10.1016/j.cplett.2010.10.040

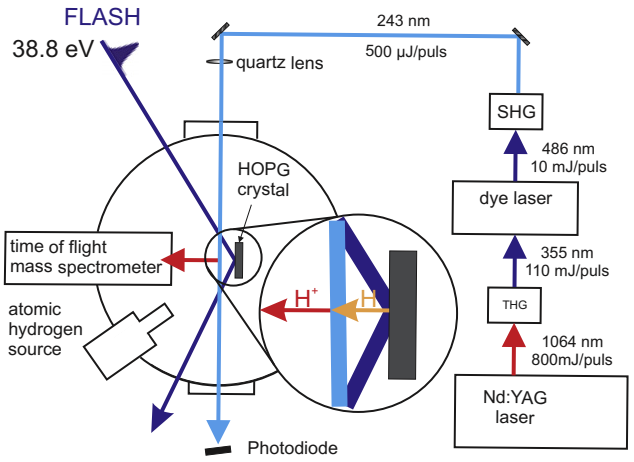

Figure 1. Scheme of the experimental set-up.

beam strikes the surface at an angle of incidence of 67.5° relative to the surface normal, see Figure 1. Due to the oblique incidence the 200×300 µm^2 ellipsoidal beam produces a 0.19 mm^2 ellipsoidal spot on the surface. An average pulse energy of 13 µJ resulting in a fluence of 6.9 mJ/cm^2 is thus applied. At this wavelength the reflectivity of graphite amounts to R = 43.4%, and therefore a fluence of 3.9 mJ/cm^2 is absorbed by the sample. The penetration depth of the radiation is about 5.08 nm [10].

Desorbing hydrogen atoms are detected in the gas phase by (2 + 1) resonantly enhanced multi photon ionization (REMPI) via two-photon absorption in the $2s^2S_{1/2} \leftarrow 1s^2S_{1/2}$ transition. The detection laser system consists of a frequency tripled Nd:YAG laser (Quanta Ray, GCR-170) pumping a commercial dye laser system (Sirah, Cobra Stretch, $\Delta\tilde{\nu} = 0.06$ cm^{-1}, $\lambda \sim 486$ nm, 10 mJ/pulse). The output is frequency doubled in a BBO crystal to produce radiation around 243 nm for the two-photon excitation. The detection laser runs in a toggle mode with 10 Hz, recording signal and background separately. H^+ photo ions are detected by a Wiley–McLaren type time-of-flight mass spectrometer. This device is also capable to detect ions directly desorbed by the FLASH pulse [11]. It should be mentioned that a detuning of the probe laser wavelength from the $2s^2S_{1/2} \leftarrow 1s^2S_{1/2}$ two-photon resonance caused a complete cease of the H^+ ion signal. The signal observed can thus unambiguously attributed to originate from H atoms desorbing in the electronic ground state. The output of the microchannel plates is monitored on a digital oscilloscope, gated and forwarded to a computer. The ionization of the neutral H atoms occurs after a defined flight path of 7 mm and a defined time delay with respect to the desorbing XUV pulse. By changing the delay between FLASH and the detection laser the kinetic energy of neutral desorbing molecules can be inferred, under the assumption of a prompt desorption. At each time setting about 500 pulses are summed and averaged.

3. Results and discussion

Figure 2a shows the raw data of hydrogen atoms desorbing from the graphite surface as detected by changing the time delay between desorption and detection laser up to about 75 µs. In Figure 2b the resulting velocity distribution is shown, after converting the arrival time distribution of Figure 2a into a flight time and then by a Jacobi transformation into the velocity distribution. The open circles represent the experimental data points. The distribution peaks at a comparatively low velocity of about 380 ms^{-1} with additional shoulders at even lower velocities of about 250 ms^{-1} and 120 ms^{-1}. A second distinct maximum at 1000 ms^{-1} and a

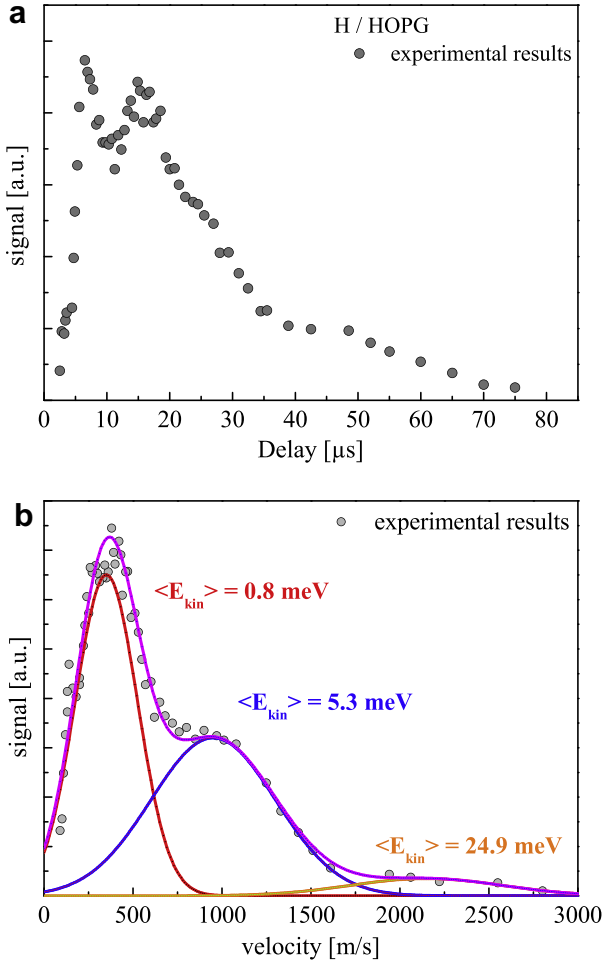

Figure 2. (a) Arrival time distribution of neutral H atoms desorbing from graphite (0001). Flight distance to detection $\Delta L = 7$ mm, desorption wavelength $\lambda_{des} = 32$ nm, surface temperature $T_s = 300$ K. (b) Converted velocity distribution of the neutral H atoms from graphite ($h\nu = 38.8$ eV).

third weak feature around 2200 ms^{-1} can be discerned. The solid curves represent Gaussian velocity distributions fitted to the experimental data. From these fitted distributions the average kinetic energies can easily be obtained. The Gaussian approximations for the three easily discernable components yield average kinetic energies of $\langle E_{kin} \rangle = 0.8$ meV, 5.3 meV, and 25 meV for hydrogen atoms with velocities of 380 ms^{-1}, 1000 ms^{-1}, and 2200 ms^{-1}, respectively. These are evidently very low kinetic energies. Fast hydrogen atoms which can be associated with a direct desorption from a repulsive H-graphite electronic state are not observed. To identify the kinetic energies of atoms desorbing directly from the exited state a knowledge about this potential is essential. Since further the lifetime of the exited electronic state seems to be less than a femtosecond, the probability to observe such atoms is very low, and therefore escapes our detection sensitivity.

Without redosing the surface and desorbing always at the same surface spot an exponential decrease of the signal is observed. Since the fluence dependence of the signal depends linearly on the desorption laser pulse energy one can deduce an effective desorption cross section from such a measurement. Observing this signal for more than 500 pulses which results in a total applied/absorbed fluence of 1.95 J/cm^2 or 5.6×10^{17} photons per cm^2 one arrives at a desorption cross section of $\sigma = 1.3 \times 10^{-19}$ cm^2. A desorption yield of about 3×10^{-5} ML per XUV pulse is observed. For the velocity distribution shown in Figure 2 only about 2000

pulses are accumulated at the same surface spot. Then another spot is chosen. Data for the same delay but different surface spots are averaged.

For a theoretical description of the neutral atomic kinetic energy spectrum we employ electron scattering theory in conjunction with density functional theory (DFT). The adsorbed atom is described by an adiabatic potential $V_0(z)$, where z denotes the desorption coordinate, as shown in Figure 3. The corresponding Hamiltonian is described by H_0. The electronic system comprising both the adsorbate and the substrate is described by a Newns–Anderson type Hamiltonian H_{NA} featuring a normally unoccupied resonant electronic state $|a\rangle$, localized near the hydrogen atom. When $|a\rangle$ becomes occupied by hot electron scattering the electronic structure changes and the Born–Oppenheimer potential of the adsorbate changes to an excited state potential $V_1(z)$ The state $|a\rangle$ is therefore connected with an interaction Hamiltonian H_I which couples the pure electronic term H_{NA} with the adsorbate Hamiltonian H_0. Even when the state $|a\rangle$ is only short-lived, a transient population disturbs the system and may induce transitions between bound vibrational states within V_0 or from a bound to a desorbed state. The total Hamiltonian of the system is then

$$H = H_{NA} + H_0 + H_I. \tag{1}$$

The adsorbate Hamiltonian in the electronic ground state is given by

$$H_0 = \frac{1}{2}m\dot{z}^2 + V_0(z), \tag{2}$$

The Newns–Anderson Hamiltonian of the electronic system is described by

$$H_{NA} = \varepsilon_0 c_a^\dagger c_a + \sum \epsilon_q c_q^\dagger c_q + \sum \left(V_{aq} c_a^\dagger c_q + V_{aq}^* c_q^\dagger c_a\right), \tag{3}$$

and the interaction term is

$$H_I = \varepsilon_a(z) c_a^\dagger c_a - \epsilon_0 c_a^\dagger c_a. \tag{4}$$

In these expressions $\epsilon_a(z) = V_1(z) - V_0(z)$ gives the vertical excitation energy between the ground and excited state potentials, $c_a^\dagger$ and $c_q^\dagger$ are creation operators for the resonant state $|a\rangle$ and the substrate states $|q\rangle$, respectively, and $\epsilon_0 = \epsilon_a(z=0)$ [12,13]. The dynamics of the system is thus given by the motion on $V_0(z)$ when the state $|a\rangle$ is unoccupied, and on $V_1(z)$ when the electronically resonant state is occupied. In the next step the resonance is assigned a Lorentzian width Γ, and the interaction Hamiltonian is expanded around the ground state minimum yielding $H_I = -f_a z c_a^\dagger c_a$, where f_a denotes the force felt by the adsorbate when the resonance $|a\rangle$ is occupied.

The differential probability $dP_n(k)$ that a hot electron with energy ϵ_i will induce a transition from a bound state $|n\rangle$ of the adsorbate to a free state $|k\rangle$ can be calculated in second order perturbation theory [14]. Asymptotically, the free states become plane waves and therefore can be converted into velocities.

The scattering probability into a free state $|k\rangle$ is calculated to be [7]

$$dP_n(k) = \frac{f_a^2\Gamma^2}{(E_k - E_n)^2}|\langle k|z|n\rangle|^2 dk \times \left|\frac{1}{\varepsilon_i - \varepsilon_0 + i\Gamma/2} - \frac{1}{\varepsilon_i - \varepsilon_0 - (E_k - E_n) + i\Gamma/2}\right|^2, \tag{5}$$

where E_n and $E_k = \hbar^2 k^2/2m$ are eigenenergies of bound and free states, respectively.

As has been shown previously [7], this expression allows one to calculate the contribution of each vibrational state in the bound potential to the kinetic energy distribution of the desorbed atoms. The parameters and potentials have been calculated with GPAW which is a grid-based DFT code using the projector augmented wave method. [15] The excited potential energy is obtained from a delta self-consistent field (ΔSCF) method, [16] where an antibonding C–H orbital is taken as the resonant state $|a\rangle$. The ground state atomic adsorption potential shows no barrier for the para, and one of $E_b = 180$ meV for the ortho configuration [4,5]. These potentials are approximated by Morse potentials with $V_0(z) = D[e^{-2\alpha z} - 2e^{-\alpha z}]$. For the para configuration $D = 1.97$ eV and $\alpha = 3.57$ Å^{-1}, for the ortho $D = 2.1$ eV and $a = 3.5$ Å^{-1} are used. The coupling parameters f are obtained from the excited state potential energy $V_1(z)$ and gives $f = 0.27$ eV/Å for the para state and $f = 0.57$ eV/Å for the ortho state. It turns out that at the high coverages of 0.1 ML used in the present experiment another adsorption configuration is of importance. When all adsorbed H atoms show a para configuration with respect to each other, a so-called uniform para configuration as shown in Figure 4, the individual binding

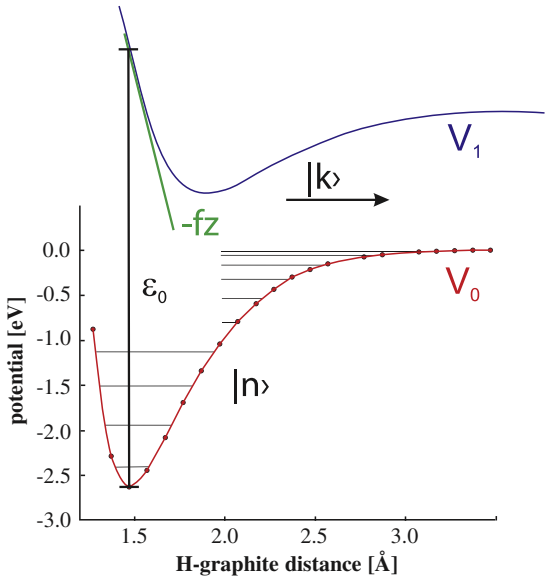

Figure 3. Illustration of the ground and excited state potentials V_0 and V_1 as a function of the hydrogen distance z from the slab. The ground state potential has a number of discrete bound states $|n\rangle$ and a continuum of free states $|k\rangle$. The excited state $V_1(z)$ mediates the non-adiabatic coupling, which allow hot electrons to induce transitions between the bound and continuum states of V_0. In the model Eq. (5), we have approximated the coupling by the first order Taylor expansion of the excited potential $-fz$.

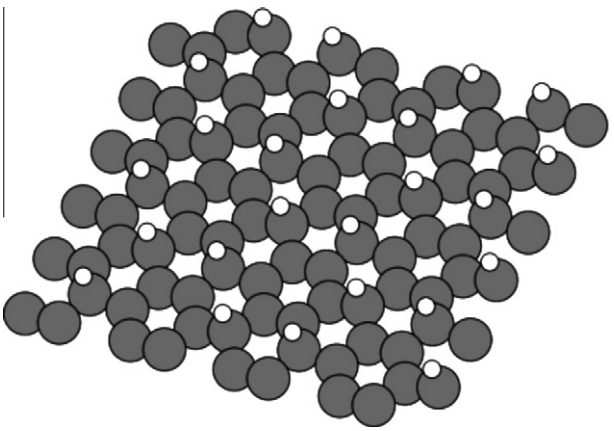

Figure 4. Model of the uniform para configuration of adsorbed hydrogen atoms on graphite. All nearest neighbor H atoms are in a para configuration with respect to each other. This yields an even larger binding energy of $E_b = 2.7$ eV than the dimer para configuration of $E_b = 1.97$ eV. Also in this case the adsorption into a free para state is barrier free.

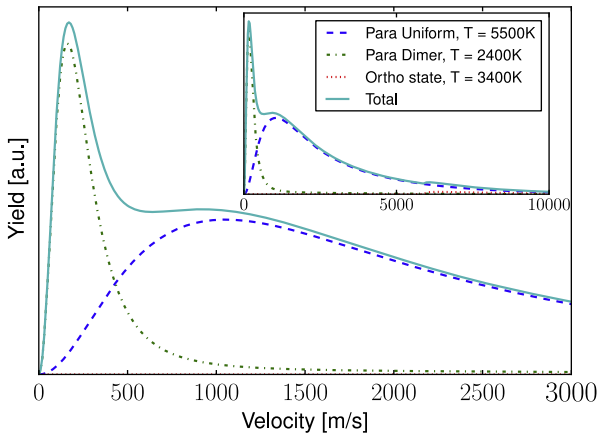

Figure 5. Theoretical velocity distribution of H atoms desorbing from graphite. The dashed green line is associated with desorption out of the dimer para state, the dashed blue line out of the uniform para configuration, and the dot-dashed red line out of the ortho state (inset) which appears above 6000 ms^{-1}. (For interpretation of the references to colour in this figure legend, the reader is referred to the web version of this article.)

energy increases to even $E_b = 2.7$ eV, again with no barrier for a further adsorption into (or desorption from) another para site. The corresponding Morse potential is then parameterized by $D = 2.7$ eV, $\alpha = 3.5$ $Å^{-1}$ and $f = 0.37$ eV/Å. In Figure 3 the red line denotes the V_0 state for a uniform para Morse potential with respective vibrational states. The potential is significantly narrower than a C–H bond gas phase potential. It should be mentioned, that the exited state V_1 is estimated and serves only as an illustration.

To calculate the desorption yield at a given velocity, we need to sum up all $dP_n(k)$ weighted by the probability that the adsorbate is in the vibrational state $|n\rangle$. The vibrational population distribution is the result of interactions with multiple hot electrons. We will assume that this distribution can be described by a vibrational temperature, which is taken as a fit parameter of the theoretical velocity distributions to the experimentally observed one. Figure 5 shows the calculated velocity distribution. The dash-dotted green curve describes the velocity distribution of H atoms expected for electron scattering on the last vibrational state of atoms in the para dimer configuration. The distribution peaks at about 170 ms^{-1}. The dashed blue curve shows the velocity distribution expected from the uniform para distribution with a peak yield at about 1000 ms^{-1}. Desorption out of the ortho dimer configuration contributes only minor to the yield, barely visible in the inset of Figure 5 at velocities above about 6000 ms^{-1}. These velocity distributions are obtained for high vibrational temperatures of the still bound H atom before a final electron scattering event excites them into the repulsive electronically excited state. For the uniform para configuration the vibrational temperature obtained amounts to $T_{vib}(\text{para, uniform}) = 5500$ K, that for the dimer para configuration to $T_{vib}(\text{para, dimer}) = 2400$ K, and for the ortho $T_{vib}(\text{ortho}) = 3400$ K. The relative yields for desorption out of different adsorption sites are 1: 4.1: 0.1 for the para dimer, uniform para and ortho dimer states, respectively. The theoretical velocity distribution qualitatively fit the experimentally observed one.

The model calculation demonstrates that at the relatively high coverages chosen in the experiment large patches of uniform para configurations must be present on the graphite surface. Further, the required vibrational temperatures are significantly higher than in a previous experiment [7] where the desorption is initiated by near-UV excitation with a photon energy of about $h\nu = 3.1$ eV. This latter finding can be rationalized since the high XUV photon energy of about 38.8 eV results in a significantly hotter electron distribution which in turn excites the bound H–Carbon vibration to a larger extent. Slightly different vibrational temperatures for the different adsorption configurations are also to be expected, because the electron scattering rate critically depends on the vibrational potential. Not only the overlap of the vibrational wave function enters via the Franck–Condon factor into the calculation, also the differences in the vibrational level spacing.

In summary, the experimental observation of a structured velocity distribution for desorbing neutral H atoms from graphite, initiated by XUV pulses from a free-electron laser, can well be understood with the results from a model calculation based on first principles. The different velocity peaks are the result of desorption out of different adsorption sites with different potential energies. These energies are determined by the lateral hydrogen interactions on the surface. Patches of uniform para configurations contribute significantly to the total yield.

Acknowledgments

The authors gratefully acknowledge technical contributions by S. Eppenhoff and the mechanical workshop of the University Münster. For helpful collaboration we want to thank the FLASH team at HASYLAB and acknowledge partial financial support by the Bundesministerium für Bildung und Forschung via Grant No. 05 KS4PMC/8.

References

[1] D.A. Williams, E. Herbst, Surf. Sci. 500 (2002) 823.
[2] X. Sha, B. Jackson, Surf. Sci. 496 (2002) 318.
[3] N. Rougeau, D. Teillet-Billy, V. Sidis, Chem. Phys. Lett. 431 (2006) 135.
[4] L. Hornekær et al., Phys. Rev. Lett. 97 (2006) 186102.
[5] L. Hornekær et al., Phys. Rev. Lett. 96 (2006) 156104.
[6] Ž. Šljivančanin, E. Rauls, L. Hornekær, X. Xu, F. Besenbacher, B. Hammer, J. Chem. Phys. 131 (2009) 084706.
[7] R. Frigge et al., Phys. Rev. Lett. 104 (2010) 256102.
[8] W. Ackermann et al., Nature Photonics 1 (2007) 336.
[9] R. Mitzner et al., Phys. Rev. A 80 (2009) 025402.
[10] B.L. Henke, E.M. Gullikson, J.C. Davis, At. Data Nucl. Data Tables 54 (2) (1993) 181.
[11] B. Siemer, T. Hoger, M. Rutkowski, R. Treusch, H. Zacharias, J. Phys.: Condens. Mat. 22 (2010) 084013.
[12] N.S. Wingreen, K.W. Jacobsen, J.W. Wilkins, Phys. Rev. B 40 (1989) 11834.
[13] T. Olsen, J. Gavnholt, J. Schiøtz, Phys. Rev. B 79 (2009) 035403.
[14] T. Olsen, Phys. Rev. B 79 (2009) 235414.
[15] J.J. Mortensen, L.B. Hansen, K.W. Jacobsen, Phys. Rev. B 71 (2005) 035109.
[16] J. Gavnholt, T. Olsen, M. Engelund, J. Schiøtz, Phys. Rev. B 78 (2008) 075441.